

Article - Engineering, Technology and Techniques

# Development of Orally Disintegrating Films HPMC-Based Containing Captopril: Mechanical, Optical and Physicochemical Studies

Larissa Aroca Colucci<sup>1</sup>

<https://orcid.org/0000-0002-3038-6499>

Leticia Norma Carpentieri Rodrigues<sup>2</sup>

<https://orcid.org/0000-0001-5175-859X>

<sup>1</sup>Universidade Metodista de São Paulo, São Bernardo do Campo, São Paulo, Brasil; <sup>2</sup>Instituto de Ciências Ambientais, Químicas e Farmacêuticas. Universidade Federal de São Paulo, Diadema, São Paulo, Brasil.

Editor-in-Chief: Paulo Vitor Farago

Associate Editor: Paulo Vitor Farago

Received: 15-Feb-2022; Accepted: 12-Jun-2022.

\*Correspondence: [leticia.carpentieri@unifesp.br](mailto:leticia.carpentieri@unifesp.br); Tel.: +55-11-4044-0500 VoIP 3576 (L.N.C.R.).

## HIGHLIGHTS

- Orally disintegrating films were prepared by solvent casting using HPMC polymer.
- Films were prepared by 3<sup>2</sup> factorial designs for oral delivery of captopril.
- Mechanical, optical, and dissolution properties were evaluated.
- The experimental design allowed to optimize the formulation.

**Abstract:** Orally disintegrating films (ODFs) comprising hydroxypropyl methylcellulose (HPMC) E6 (2%, 2.5%, and 3%) and plasticizers (glycerin [Gly], propylene glycol [PP], or polyethylene glycol [PEG]) containing CPT were prepared by the solvent casting method and characterized. The design of experiments (DoE) was used considering the amount of film-forming agent (HPMC) and the nature of the plasticizers as independent variables and thickness, mechanical properties, disintegration time, and dissolution efficiency as dependent variables. The best formulation was selected based on the desirability function ( $f_D$ ). Color analysis was performed using CIE-*Lab* coordinates. The films had a pH less than 4 and were thus suitable for maximum stability of CPT. The amount of HPMC E6 and the nature of the plasticizer play a critical role in the physical, mechanical, and physicochemical properties of the films. Principal component analysis and hierarchical cluster analysis revealed a more defined distinction of the ODFs according to their chromatic characteristics. ODFs prepared with Gly and PEG 400 were translucent, whereas the other films were transparent. DoE successfully facilitated the interpretation of the experimental data and allowed the identification of optimal values of the factors for maximum yield. The maximum value obtained for  $f_D$  was 0.8520, corresponding to 2.0 - 2.5% of the polymer (HPMC E6), and PP as plasticizer. The best-fitting kinetics model for CPT release from the ODFs was the Korsmeyer–Peppas model. The results showed that orally disintegrating films can be a promising alternative for oral administration of captopril.

**Keywords:** captopril; design of experiments (DoE); desirability function; mechanical properties; orally disintegrating film.

## INTRODUCTION

New drug delivery systems have been developed that disintegrate rapidly into the oral cavity and can be ingested without water or chewing. They are very beneficial in the treatment of patients with dysphagia, such as those who cannot swallow medicines easily, are bedridden, and geriatric and pediatric patients (young children) [1].

Hypertension is the most prevalent health problem worldwide; globally, an estimated 1.13 billion people have hypertension, most (two-thirds) belonging to low- and middle-income countries. Moreover, pediatric hypertension has increased over the last 30–40 years. Recent heart disease and stroke statistics suggest that 15% of children and adolescents have abnormal blood pressure. Although the reason for the increase in pediatric hypertension is not entirely clear, many believe it is due to the coinciding obesity epidemic [2].

Considering the risks and adverse effects induced by a hypertensive crisis, blood pressure control should be performed as soon as possible (< 1 h).

Captopril (CPT) is an angiotensin-converting enzyme (ACE) inhibitor that acts on the renin-angiotensin system by preventing the conversion of angiotensin I to angiotensin II [3], and its effect is observed 30 min after its oral administration [4]. It is considered the drug of first choice in hypertensive crisis and congestive heart failure for adults and children because of its effectiveness, low toxicity, and low cost [2]. Despite these advantages, the use of CPT in children is limited due to its low aqueous stability and the difficulty in developing a suitable dosage form.

CPT is stable in the solid state; however, in solution, it undergoes oxidative degradation with CPT disulfide dimer as the main degradation product. Its degradation in solution is complex, and depends on temperature, humidity, exposure to air, presence of hygroscopic substances, concentration, and pH, showing high stability at a pH less than 4.0 [3–7]. Available in tablet form of 12.5–100 mg for oral or sublingual administration in adults, recommended doses of CPT for children are generally less than 12.5 mg (300µg/kg/day for neonates and 6 mg/kg/day for children 1 month to 12 years), and are administered in the form of extemporaneous suspensions, which are obtained from commercially available solid dosage forms. The major problem with these extemporaneous preparations is their limited stability, which leads to problems of efficacy and tolerability. Individually packaged oral powders or capsules have been used as alternative extemporaneous preparations for administration during feeding [6].

Orally disintegrating films (ODFs) can be an innovative alternative to extemporaneous drug delivery because of their numerous advantages. Absorption of the active pharmaceutical ingredients (APIs) in this dosage form can occur in the oral mucosa (gingival, sublingual, buccal, and palatal regions) as well as in the gastrointestinal tract [8,9]. Irrespective of the route of absorption, ODFs are associated with increased bioavailability of APIs compared to conventional oral solid dosage forms, because the release occurs in the oral cavity and the dissolution of the API begins earlier [10,11]. In addition to excellent stability (as the drug in its solid state) and dosage flexibility (as solutions or suspensions for children or enteral feeding), ODFs have a small shape and size for easy placement on the tongue, where they will disintegrate instantly by saliva (< 60 s) without the need for water. In addition, their good adhesion to the oral mucosa and rapid disintegration prevents the patient from expelling or resisting its ingestion [4,12,13].

Hydrodispersible polymers are the main components of ODFs [14,15]. Polymers most commonly employed as film-forming are as follows: pullulan, hydroxypropyl methylcellulose (HPMC), hydroxyethyl cellulose (HEC), Povidone K-90, xanthan gum, tragacanth gum, guar gum, acacia gum, methyl methacrylic copolymer, carboxyvinyl copolymer, and combinations thereof. According to Mahadevaiah and coauthors [16] the addition of a plasticizer is fundamental in reducing the fragility and increasing the flexibility of ODFs. Glycerin (Gly), propylene glycol (PP), and polyethylene glycol (PEG) have excellent plasticizing properties [12]. The major limitation of the ODFs is their low drug-loading capacity (5%–30%, w/w), thereby, restricting its application with APIs employed at high doses [17]. HPMC is a water-soluble polymer that is non-ionic, biodegradable, stable over pH 3–11, and consists of cellulose ether monomers with good film-forming properties [17–20]. Ali and coauthors (2015) [21] developed ODFs containing captopril using different polymers (HPMC, PVA, PVP and carbopol 934P) and super disintegrants. Rezaee and Ganji (2018) [13] prepared ODFs of captopril employing different proportions of HPMC and pullulan, and glycerin as plasticizer.

The high efficacy of CPT in the treatment of hypertension (especially in emergencies), its low dosage, and poor stability in solutions make it a good candidate for ODFs.

There is an increasing number of published studies on the application of statistically based optimization processes in the field of pharmaceutical technology. Design of experiments (DoE) is a statistical tool capable of facilitating the interpretation of experimental data, which ultimately allows the identification of optimal factor levels for maximum performance [22,23].

In this study, ODFs of CPT were developed as an ideal alternative for its administration in children. The DoE approach was implemented to evaluate the effects of the formulation components on the physical, mechanical, and optical properties, as well as dissolution characteristics. The optimization of the responses was performed using the desirability function ( $f_D$ ).

## MATERIAL AND METHODS

### Material

Captopril (CPT) was kindly provided by Cristália Produtos Químicos e Farmacêuticos Ltda. (São Paulo, Brazil). Hydroxypropyl methylcellulose (HPMC E6 Premium LV, Dow Chimica; 4.8-7.2 mPa.s 2% in water at 20°C, 28.0-30.0% methoxyl substitution, and 7.0-12.0% hydroxypropoxyl substitution) was kindly provided by Colorcon Inc. (Cotia, São Paulo, Brazil). Glycerin (Gly), propylene glycol (PP), polyethylene glycol 400 (PEG 400) were obtained from LabSynth® (Diadema, São Paulo, Brazil). Listerine® Breath Film (Cool Mint Listerine® PocketPaks oral care strips, Pfizer - Warner-Lambert consumer healthcare division) was obtained from the pharmaceutical market. Purified water was obtained using a reverse osmosis system Gehaka model OS10LXE (São Paulo, Brazil). All other reagents were of analytical grade.

### Preparation of ODFs

ODFs were prepared using full factorial DoE approach employing two factors and three levels ( $3^2$ ) using the Statistica version 13.1 software (TIBCO Statistica Inc., CA, USA), resulting in nine formulations. The films were prepared by solvent casting method using HPMC E6 (2%, 2.5%, and 3%) as a film-forming agent, and GLY, PP, or PEG as plasticizers (10% mass polymer, w/w) [17,24]. EDTA was used as an antioxidant agent [5] (Table 1).

To prepare the formulations 25 mg of CPT was weighed, dispersed in sufficient amount of purified water, and subjected to stirring on a 10-position magnetic stirrer. Then, the plasticizer (GLY, PP, or PEG) and HPMC E6 (2%, 2.5%, or 3%) were added, and the volume was completed with purified water (q.s. to 6 mL). After 30 min, stirring was stopped, and the dispersions were kept at rest for 30 min for deaeration [25]. The dispersions thus obtained were transferred to a polystyrene mold (120x120mm, 144 cm<sup>2</sup> of area), and dried in an oven with forced air circulation and renewal (40.0 ± 0.5 °C) for 24 h. The films were removed from the molds, wrapped in an aluminum foil, and placed in a desiccator.

The amount of CPT in ODFs was calculated according to Ali [21], such that each unit of ODF (6 cm<sup>2</sup>) contains 25 mg of CPT. Films without plasticizer (F1-WP, F4-WP and F7-WP) were prepared for comparison.

**Table 1.** Composition of ODFs according to the design of experiments (DoE)

Composition	ODFs								
	F1	F2	F3	F4	F5	F6	F7	F8	F9
CPT (mg)	600	600	600	600	600	600	600	600	600
HPMC E6 LV (%)	2.0	2.0	2.0	2.5	2.5	2.5	3.0	3.0	3.0
EDTA Na (%)	0.1	0.1	0.1	0.1	0.1	0.1	0.1	0.1	0.1
<sup>1</sup> Plastificizer	GLY	PP	PEG	GLY	PP	PEG	GLY	PP	PEG
Water, q.s. (mL)	45	45	45	45	45	45	45	45	45

<sup>1</sup>equivalent to 10% of the polymer mass

### Characterization and optimization

#### Physical and mechanical properties

The thickness of the ODFs was measured in continuous mode using a Defelsko Inspection Instruments model PosiTector Standard 200 (ASTM D-6132-13) [26] with an accuracy of 0.001 ± 0.0001 µm.

The mechanical properties of the ODFs were evaluated using a puncture (ASTM D2582-16) [27] and pull-off adhesion (ASTM D4541-17) [28] tests, using a Brookfield CT3 Texture Analyzer with a 50 kg load cell. The tests were performed using the Texture ProCT software.

For the puncture test, the samples were fixed in the TA-FSF accessory, placed on the TA-BT-kit (fixture base table), and subjected to puncture strength using a TA39 probe (2 mm D, 200 mm L, stainless steel). Load vs. displacement data were recorded from the point of contact of the probe with the film until the film ruptured. The puncture strength (PS, MPA), elongation at break (E, %), and puncture to energy (PE, N/mm<sup>3</sup>) were calculated according to the method described by Radebaugh and coauthors [29]. The nature of the test did not allow the calculation of Young's modulus [25,29].

In the adhesion test, an epithelium segment of the pig oral mucosa (Animal Ethics Committee n° 1352120520) was fixed on the mucus adhesion test fixture (TA-MA) accessory, submitted in a borosilicate glass flask containing 0.9% physiological solution to reach the lower surface of the mucosa, with stirring at 37.5 °C. On the probe TA5 (12.7 mm D, 35 mm L; Black Delrin), a piece of double-sided adhesive tape was applied, and the sample was deposited on it. The parameters of hardness (H, N), adhesive force (AF, N), and adhesiveness (A, mJ) were evaluated [30]. The mechanical properties of ODFs were compared with standard film (Listerine™ Breath Film).

#### *Disintegration time*

Disintegration time was analyzed by taking film strip of 6 cm<sup>2</sup> area and employing Petri dish method. The film was placed in a petri dish containing 5 mL of simulated salivary fluid (pH 6.8 phosphate buffer). The disintegration time (DT, seconds) was noted down when the film strip was disintegrated completely. Tests were performed at room temperature. The experiment was repeated in triplicate and the mean value reported [31].

#### *Water activity ( $a_w$ ) and pH analysis*

$A_w$  was evaluated using the FA-st Water Activity Meter (GBX Instruments, France) previously calibrated with  $k_2SO_4$  ( $A_w = 0.970 \pm 0.003$ ) at room temperature. The final values, expressed as a percentage, are the averages of three measurements.

ODF(s) (F1-9) were transferred separately to Falcon (15 mL) conical tubes, where 5 mL of purified water was added, and evaluated using a pH meter (Hanna model pH21) with Ag/AgCl electrode.

#### *Surface characteristics and morphology*

The films were placed in a light booth under a daylight source (D65 lamp, 6500K) and compared visually.

#### *Scanning electron microscopy (SEM) analysis*

The morphology of the ODFs (F1-9) was evaluated using SEM JEOL model JSM-6610. The samples were fixed on a metallic support with the aid of a 12 mm thick double-sided carbon tape and subjected to metallization under vacuum to make them electrically conductive. The visualization was performed with an increase of 1.000 x with an excitation voltage of 10 – 15 kV.

#### *Optical properties*

Color determination of the ODFs was carried out using a CR-400 colorimeter (Konica-Minolta, Co. Ltd., Japan) calibrated with white backing, using standard D65 illumination and 10° absorber. The CIELAB reading system was represented by coordinates  $L^*a^*b$ , where  $L^*$ , *lightness* (0 = black, and 100 = white), and chromaticity indices: ( $a^*$ , *hue*) ( $-a = green$ ,  $+a = red$ ) and ( $b^*$ , *chroma*) ( $-b = blue$ ,  $+b = yellow$ ). The optical properties of ODFs were compared with standard polystyrene film (SPF), represented as a standard of transparency. The tests were performed in triplicates.

#### *Content uniformity*

ODFs (F1-9) were transferred to Falcon 15 mL conical tubes, 5 mL of ultra-purified water was added, stirred on a vortex-type agitator for 60 s, and filtered through filter paper. Aliquots of 100 µL were diluted 1:100 (v/v) and quantified using a Thermo Scientific spectrophotometer (Evolution 200) at 205 nm. The final values are the averages of three measurements. Content uniformity (UC, mg) results were used to calculate the amount of dissolved CPT in the dissolution profiles.

#### *Dissolution test*

Dissolution profiles were obtained using the dissolution equipment Ethik Technology model 299/TTS. A total of three units of each dosage forms (ODFs 6 cm<sup>2</sup>, CPT 25 mg) were subjected to the dissolution tests using the following conditions: Apparatus 5 (paddle over disc), stirring speed 50 rpm, medium volume 500 mL, UV spectrophotometry at 205 nm, and phosphate buffer pH 7.4 at  $37 \pm 0.5$  °C as dissolution medium [32] (Krampe and coauthors, 2016 [32]). The values obtained were expressed as percentages of captopril dissolved *versus* time.

The dissolution efficiency (DE, %) was obtained from the average dissolution profile for each formulation according to the equation (1) [33]:

$$DE\% = \left[ \int_0^T (y \times dt) / y_{100} \times (t_t - t_0) \right] \times 100 \quad (1)$$

where  $y_t$  is percent of drug dissolved at any time  $t$ ,  $y_{100}$  denotes 100% dissolution, and the integral represents the area under dissolution curve between time zero and  $T$ .

The kinetics of CPT release from ODFs was determined by finding the best fit of the dissolution data to four distinct models, zero-order (2), first-order (3), Higuchi (4) and Korsmeyer–Peppas (5), as follows:

$$Q_t = Q_0 + k_0 t \quad (2)$$

$$(\ln Q_t = Q_0 + k_1 t) \quad (3)$$

$$(Q_t = k_H t^{1/2}) \quad (4)$$

$$Q_t / Q_\infty = k_{KP} t^n \quad (5)$$

where  $Q_t$  is the amount of drug released at time  $t$ ,  $Q_0$  the amount of drug in the solution at  $t = 0$  (usually,  $Q_0 = 0$ ,  $Q_\infty$  the total amount of drug in the matrix, and  $Q_t / Q_\infty$  the fraction of drug released at time  $t$ . In these equations,  $k_0$  is the zero-order release constant (2),  $k_1$  is the first-order kinetic constant (3),  $k_H$  represents the Higuchi rate constant (4),  $k_{KP}$  is the Korsmeyer–Peppas dissolution rate constant and the  $n$  is the release exponent (5).

The application of the Korsmeyer–Peppas model was limited to data on a maximum of 60% of the accumulated amount of released drug. The model that best fits the CPT release data was selected based on the correlation coefficient ( $r$ ) value of various models [34].

## Data processing

Statistical version 13.1 software (TIBCO Software Inc., CA, USA) was used for the statistical analysis of the data. The results of thickness, disintegration time, mechanical properties and dissolution efficiency were analyzed using DoE for the models without interaction, and with two-level interactions, (linear, linear) or (linear, quadratic). Based on the correlation coefficient (R-sqr) and adjusted R-sqr (Adj) and p-value, the best-fitted models for each response were chosen. The desirability method was used to optimize the formulations [35]. Principal component analysis (PCA) was used to explain the optical properties of CIELAB.

## RESULTS AND DISCUSSION

The results of the physical, physicochemical, and mechanical properties obtained for ODFs prepared with (F1-9) and without plasticizers (F1-WP, F4-WP and F7-WP), and standard film (Listerin® Breath Film) are presented in Tables 2 and 3.

### Optimization of factors by DoE

DoE is a statistical technique used to plan experiments and analyze data using a controlled set of tests designed to model and explore the relationship between factors and observed responses [22].

**Table 2.** Average values (and standard deviation) of physical and physicochemical properties obtained for ODFs with (F1-9) and without plasticizers (F1-WP, F4-WP and F7-WP), and standard film (Listerin® Breath Film) (n=3)

Parameters	Thickness, $\mu\text{m}$	pH	DT, sec.	$a_w$ , %	UC, mg	DE, %
Standard film	39.44±1.20	5.43±0.12	41±2.87	0.07±0.03	NA	NA
F1-WP	62.80±3.34	2.70±0.01	45±0.89	0.677±0.01	NA	NA
F4-WP	93.50±2.15	2.70±0.05	52±1.12	0.633±0.01	NA	NA
F7-WP	128.83±3.79	2.74±0.04	72±0.95	0.611±0.05	NA	NA
F1	63.90±1.79	3.65±0.15	45.33±1.25	0.779±0.02	25.11±1.22	75.62±0.42
F2	46.10±2.47	4.05±0.25	49.67±1.70	0.784±0.01	24.87±2.56	82.85±1.02
F3	63.47±7.35	3.85±0.09	46.67±0.47	0.805±0.00	25.75±1.02	79.00±0.33
F4	78.93±14.51	3.53±0.05	54.00±3.27	0.803±0.01	25.98±2.47	73.38±0.09
F5	91.23±10.77	3.47±0.07	54.33±1.25	0.794±0.01	24.91±1.12	87.00±0.37
F6	87.07±12.70	3.58±0.05	53.67±2.87	0.797±0.01	25.55±1.07	67.27±0.40
F7	104.63±17.96	3.42±0.02	65.33±3.86	0.794±0.01	24.68±1.49	71.78±0.32
F8	121.20±37.46	3.42±0.08	67.67±2.05	0.796±0.00	25.87±0.97	83.77±0.79
F9	98.30±7.85	3.67±0.08	69.67±3.30	0.808±0.00	25.65±1.32	68.21±0.76

DT, disintegration test;  $a_w$ , water activity; UC, uniformity content; DE, dissolution efficiency. NA, not applied

**Table 3.** Average values (and standard deviation) of mechanical properties obtained for ODFs with (F1-9) and without plasticizers (F1-WP, F4-WP and F7-WP), and standard film (Listerin® Breath Film) (n=3)

Parameters	D, mm	Puncture test			Adhesive test		
		PS, MPA	E, %	PE, N/mm <sup>3</sup>	H, N	AF, N	A, mJ
Standard film	0.70±0.07	1.12±0.16	1.16±0.25	0.30±0.04	4213±136	70.00±7.07	2.70±0.16
F1-WP	4.23±0.16	94.43±25.21	36.50±2.30	79.83±53.88	1333±112	15.00±6.02	0.10±0.08
F4-WP	3.75±0.27	215.39±51.58	29.78±3.64	153.78±40.34	2618±103	18.33±5.23	0.57±0.05
F7-WP	3.55±0.14	287.54±114.36	26.98±1.91	140.49±55.04	3732±154	35.00±23.45	1.20±0.11
F1	1.90±0.26	1.60±0.22	8.69±2.30	0.88±0.10	549±83	15.00±6.12	0.20±0.07
F2	1.46±0.29	2.99±0.73	5.32±1.99	1.75±0.58	573±78	15.00±5.01	0.20±0.03
F3	1.82±0.06	1.51±0.37	7.87±0.51	0.89±0.29	555±65	16.67±5.04	0.23±0.04
F4	1.75±0.16	2.24±0.49	7.37±1.34	0.87±0.08	1200±102	46.67±7.12	0.37±0.12
F5	1.34±0.31	3.35±1.26	4.57±2.04	0.79±0.34	1472±87	48.33±4.12	0.57±0.09
F6	1.95±0.25	1.96±0.46	9.12±2.18	0.83±0.18	1737±114	45.00±3.72	0.67±0.06
F7	1.64±0.39	2.96±1.14	6.75±3.10	0.74±0.25	2470±120	60.00±6.45	1.18±0.10
F8	1.36±0.23	3.60±0.66	4.61±1.49	0.81±0.47	2195±106	65.00±4.54	1.10±0.07
F9	1.84±0.19	2.34±0.19	8.10±1.53	0.80±0.17	1922±98	53.33±5.48	1.20±0.08

D, displacement; PS, puncture strength; E, elongation at break; PE, puncture to energy; H, hardness (cycle I); AF, adhesive force; and, A, adhesiveness

#### *Effect on thickness and disintegration time*

The thickness of ODFs is important in achieving convenient dosage form administration and is related to the amount of polymer and drug present in the preparation. It is known that the amount of plasticizer can slightly increase the thickness of ODFs [25].

The thickness identified in this study agreed with the ideal values described in the literature [25] and the high standard deviations observed in some ODFs could be attributed to the equipment used for ODF drying, where the irregularity of the tray level prevented the homogeneous distribution of the dispersions in the molds (Table 2).

According to Takeuchi and coauthors [31], the Petri dish method has the advantage of enabling close observation of how the strip disintegrates. However, in this method, the film strip floats on the surface of the medium without stirring; thus, the mechanical force of the tongue during disintegration in the oral cavity acting on the films is not simulated (Table 2).

For both parameters, thickness ( $R^2 = 0.87931$ ; Adj: 0.67815) and disintegration time ( $R^2 = 0.98757$ ; Adj: 0.96685), only the polymer variable (linear) showed a significant effect ( $p < 0.05$ ), and the parameters increased as a function of the amount of polymer (HPMC) present in the formulations.

#### *Effect on mechanical properties*

ODFs must have adequate mechanical strength to resist handling without suffering damage and have enough tension to be easily removed from the mold after drying but must not be so flexible as to elongate during cutting and packaging, compromising the content uniformity of pharmaceutical units [10].

Although stress-strain testing is commonly used in the evaluation of ODFs, it presents limitations because it is designed for ductile materials; therefore, having limited sensitivity to polymers [29]. Puncture testing consists of an alternative method to evaluate the mechanical properties of ODFs capable of overcoming these disadvantages [25].

The ODFs prepared without plasticizers were harder and more brittle for extrusion (Figure 1A); however, the addition of plasticizers made the dosage form softer and flexible, facilitating the removal of molds (Figure 1B).

In the puncture test, the two-level interaction model (linear, linear) was the most appropriate for all parameters evaluated (Table 3). For the puncture strength ( $R^2 = 0.98224$ ; Adj: 0.95263), both the polymer (linear) and plasticizer (quadratic) had a significant influence ( $p < 0.05$ ), as the puncture strength increased with polymer concentration, and the effect of plasticizer obeyed the following order: PP > Gly > PEG; for elongation at break ( $R^2 = 0.96734$ ; Adj: 0.88623), only the plasticizer variable (quadratic) exhibited a significant influence ( $p < 0.05$ ) and the ductility of the films increased in the following order: PEG > Gly > PP. In addition, the puncture energy ( $R^2 = 0.54872$ ; Adj: 0) was not significantly influenced by the amount of polymer and nature of the plasticizer. As shown in Table 3 and Figure 1B, the values of the puncture test for the standard film (area of the hatched part) were lower than those observed for the test films.

The elongation at break is a measure of polymer ductility. Plasticizers decrease the molecular attraction between adjacent polymer chains, increase the mobility between molecules, decrease the glass transition temperature, and improve polymer flexibility and elasticity. For this reason, films prepared with plasticizers deform more than films prepared without plasticizers [16,25].

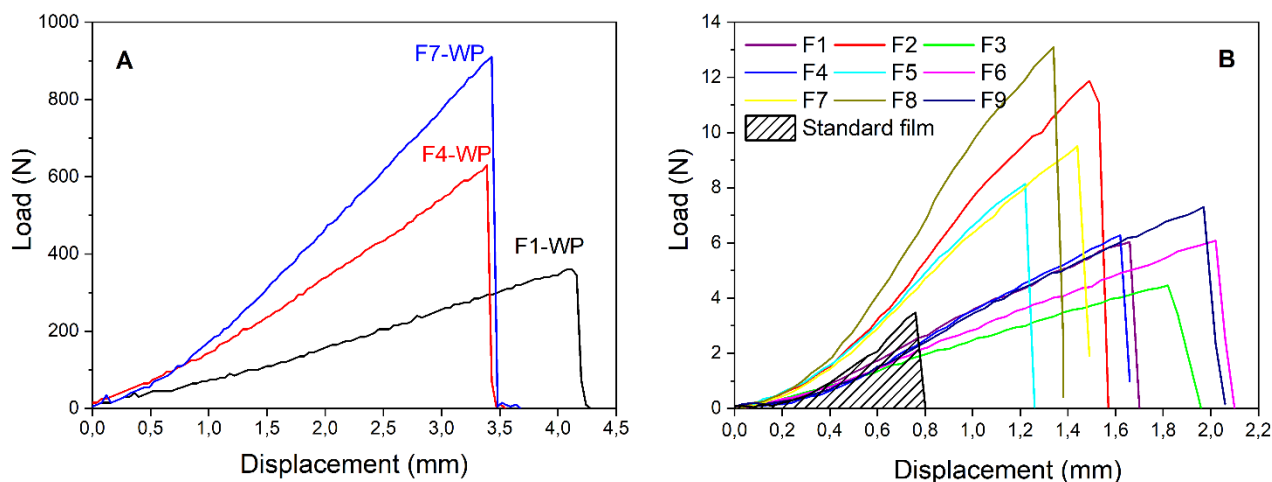


**Figure 1.** Curves obtained for ODFs without plasticizers (F1-WP, F4-WP and F7-WP) (A), ODFs with plasticizers (F1-9) and standard film (Listerin® Breath Film, cross-hatched area) (B), by means of puncture test

The physicochemical properties of the plasticizers, such as chemical structure, shape, polarity, chain length, physical state, and number of active functional groups determine their ability to plasticize a polymer network. The differences in the plasticizer effect can be attributed to the varying availability of oxygen atoms for the hydrogen bond. For instance, the spacing of the oxygen atoms in PEG allows more room for the formation of hydrogen bonds with biopolymer chains [37].

Mahadevaiah and coauthors [16] evaluated the addition of PEG (0.01 - 0.04%) or Gly (0.01 - 0.05%) to HPMC E6 Premium LV films (5%) and found that the addition of plasticizers decreased the Young's modulus and tensile strength, and that Gly was a more efficient plasticizer than PEG.

The use of a plasticizer can overcome the brittleness and soften the rigidity of the film structure by reducing the intermolecular forces. However, the use of an excessive amount of plasticizer can decrease the adhesive strength of the films by over-hydrating the film formulations [25].

Oral mucosal adhesion is a specific term used to describe the interaction between the oral mucosa and the polymeric matrix. Important variables in this process are the coefficient of diffusion of the polymer in the mucin layer and the contact time between the polymer and the mucosa [19]. The mechanisms that govern mucoadhesion are determined by the intrinsic properties of the formulation and the medium applied. In general, non-ionic polymers have lower mucoadhesive strength than ionic polymers (anionic or cationic). Although weak, non-ionic polymers can exhibit bioadhesive properties through non-covalent interactions with the surrounding fluids [8,25,30]. Most ODFs are not necessarily designed to be mucoadhesive; however, they may exhibit some degree of mucoadhesiveness because of the inherent characteristics of the polymers used [8].

In the adhesive test, the two-level interaction model (linear, linear) was the most appropriate for all parameters evaluated (Table 3). For hardness ( $R^2 = 0.94963$ ; Adj: 0.86567) and adhesiveness ( $R^2 = 0.97811$ ; Adj: 0.94163) the polymer variable (linear) showed significant influence ( $p < 0.05$ ), and for adhesive force ( $R^2 = 0.99076$ ; Adj: 0.97535) the polymer variable (linear, quadratic) had a significant effect ( $p < 0.05$ ). However, all parameters (hardness, adhesiveness, and adhesive force) increased proportionally with the polymer concentration (HPMC) (Table 3, Figure 2B).

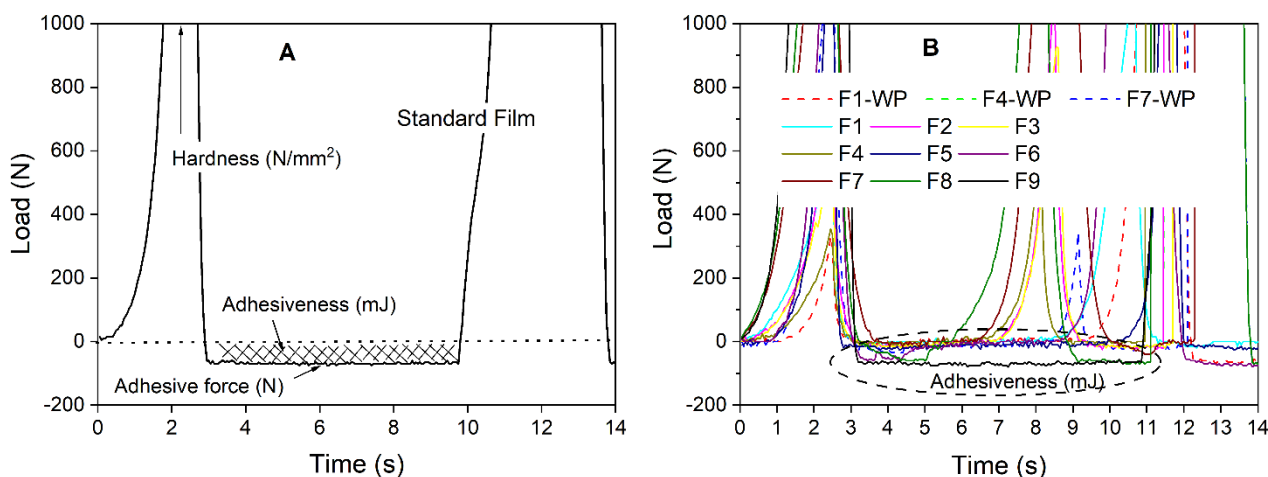


**Figure 2.** Curves obtained for standard film (Listerin® Breath Film) (A), and ODFs without plasticizers (F1-WP, F4-WP and F7-WP) and with plasticizers (F1-9) (B), by means of adhesive test

The standard film (Listerine® breath film) showed high values for hardness, adhesive strength, and adhesiveness (Figure 2A). Pullulan is the main film-forming polymer of the Listerine® breath film; however, it also contains xanthan gum and carrageenan. Pullulan is a modified starch with good film-forming properties and is one of the preferred polymers used in the preparation of oral polymeric matrices, but its low availability results in high-cost pullulan products. Therefore, pullulan is normally mixed with other more abundant and less expensive compatible polymers. Anionic polymers can naturally be used as bioadhesive materials because they tend to adhere to the mucosa through non-covalent secondary interactions, normally hydrogen bonds between the charged polymer chains and the oligosaccharide side chains of mucosal proteins. Xanthan gum is an anionic polysaccharide with exceptional mucosal adhesive properties, formed by 1,4-linked residues  $\beta$ -D-glucose with a trisaccharide chain linked to alternating D-glucosyl residues. Additionally, carrageenans constitute a group of anionic polymers that are widely used for the formation of ODFs, owing to their excellent mucosal-adhesive properties; they contain sulfated functional groups capable of forming non-covalent bonds with the lateral chains of the oligosaccharides of mucosal proteins [8].

## Characterization of ODFs

### Water activity ( $a_w$ ) and pH analysis

The pH and  $a_w$  are related to the development of microorganisms, enzymatic activity, and product stability (Table 2). The films showed pH less than 4.0 which is suitable for CPT stability [3–7].

As a measure of the energy state of the water in a system,  $a_w$  is a more effective indicator of microbial stability than humidity. As such, the importance of  $a_w$  is related to the stability of the final product [30]. All ODFs showed  $a_w$  above the optimal conditions to inhibit microbial growth ( $a_w > 0.70$ ); therefore, the use of preservatives is recommended.

### Surface characteristics and morphology

A slight color difference was observed between ODFs. Visual evaluation revealed that the films prepared with Gly (F1, F4, and F7) and PEG 400 (F3) were translucent, whereas the films were transparent (Figure 3) [36]. ODFs prepared with Gly (F1) or PEG 400 (F3) in combination with low concentrations of HPMC E6 (1.5%) exhibited the presence of fat droplets dispersed in the systems, suggesting greater difficulty in concentration (Figure 4).

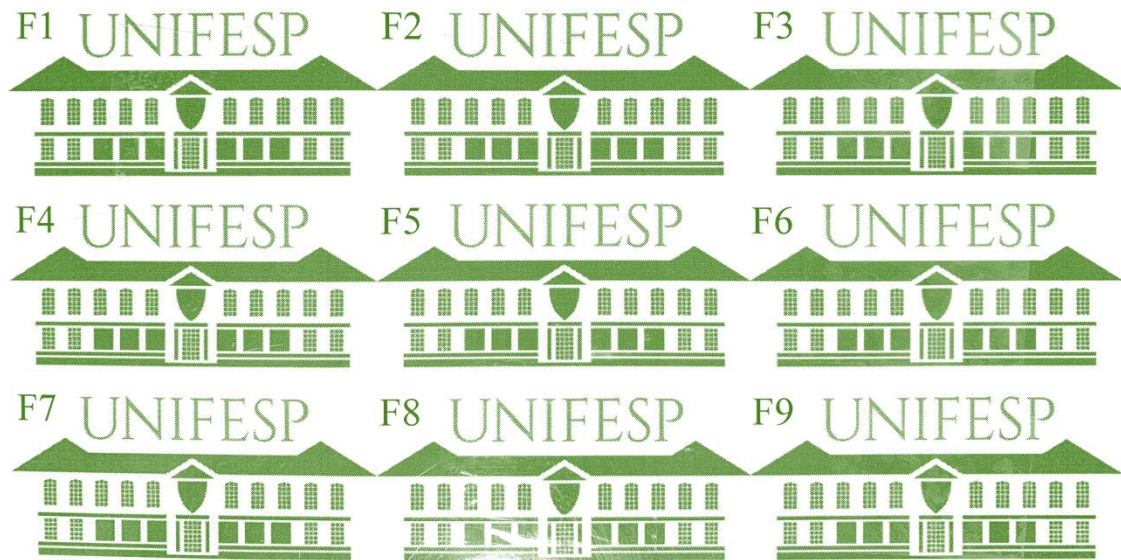


**Figure 3.** Visual transparencies of ODFs (F1-9)

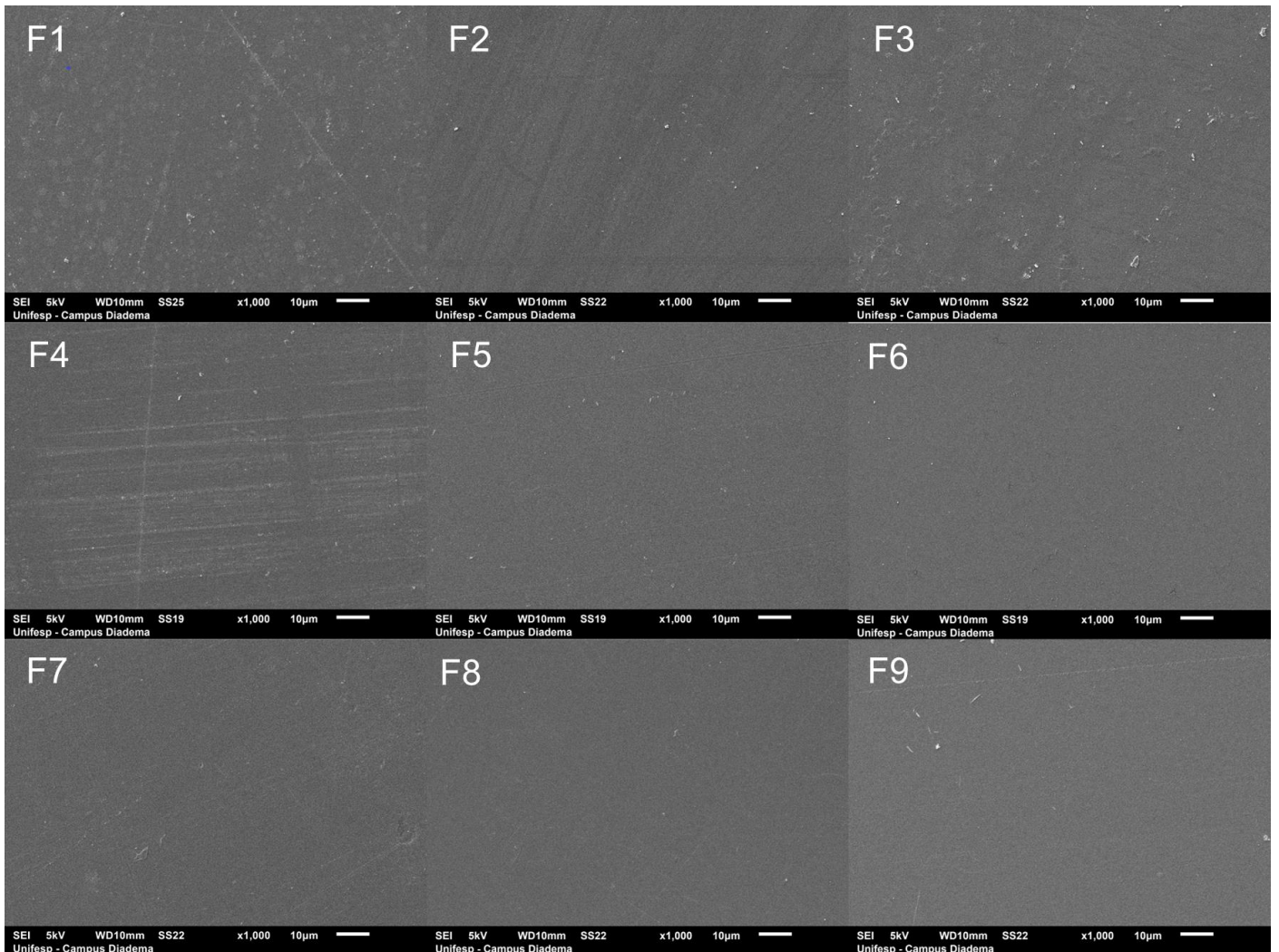


**Figure 4.** Photomicrographs of ODFs obtained through Jeol scanning electron microscope (SEM) with 1.000x magnification

### Optical properties

The CIELAB color space is widely used currently in industry to detect small differences in color [38].

The  $L^*$  coordinate indicated high luminosity in the samples, the chromatic coordinate  $a^*$  was assumed to be negative relative to green, and the  $b^*$  coordinate had positive values relative to yellow (Table 4).

The first two principal components were selected from the observed eigenvalues (Table 5). The eigenvalues are formed by coefficients that correspond to the relative weight of each variable in the principal component and are used to calculate the principal component scores. The higher the absolute value of the coefficient, the more important is the corresponding variable in the component calculation. Based on the values of the coefficients found for the eigenvectors, it was possible to observe that the first principal component (PC1) (6) had a negative association with  $b^*$ , and a positive association with  $a^*$ , while the second principal component (PC2) (7) was positively associated with  $L^*$  and  $a^*$  (Table 5):

$$\text{PC1: } -0.4068 L^* + 0.5924 a^* - 0.6953 b^* \quad (6)$$

$$\text{PC2: } +0.8399 L^* + 0.5423 a^* - 0.0292 b^* \quad (7)$$

Principal component analysis (PCA) was employed to identify the interrelationship among the variables (Table 5, Figure 5A), and the hierarchical cluster analysis (HCA) allowed grouping the samples according to similarity (Figure 5B).

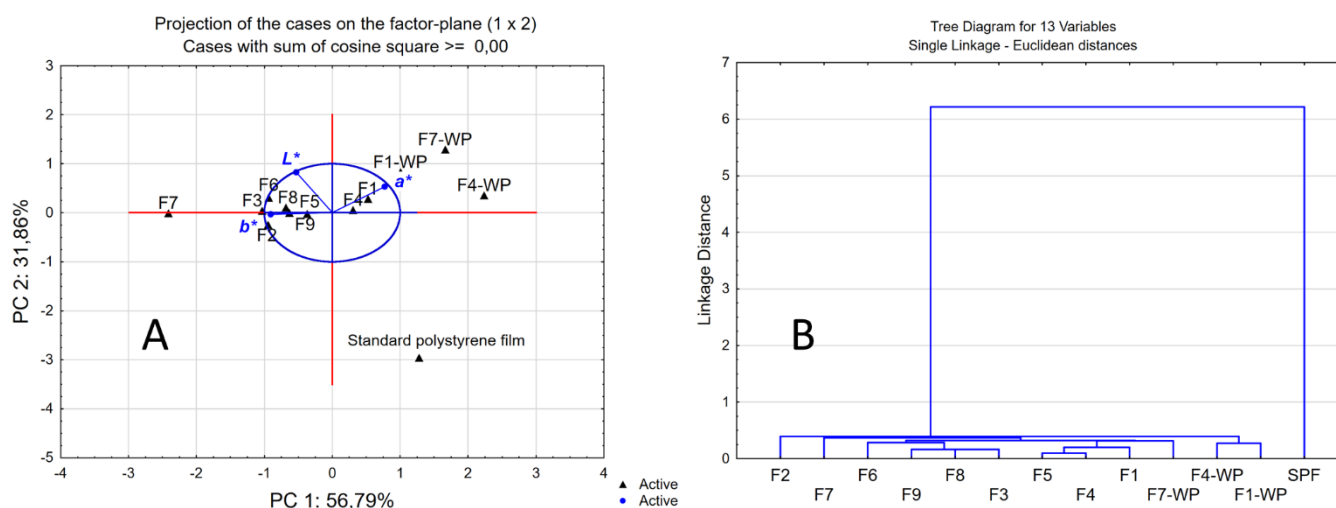


**Figure 5.** (A) PCA: Bi plot of the samples in the space defined by the first two principal components; (B) HCA: Hierarchical cluster analysis obtained for the samples (SPF and ODFs) using CIELAB color space

**Table 4.** Mean values and standard deviation of the chromaticity coordinates obtained for CIELAB color space

Samples	$L^*$	$a^*$	$b^*$
SPF	96.44±0.08	-0.96±0.02	2.84±0.03
F1-WP	102.84±0.08	-0.62±0.09	2.91±0.57
F4-WP	102.64±0.42	-0.54±0.09	2.74±0.52
F7-WP	103.35±0.40	-0.55±0.04	2.76±0.44
F1	103.40±0.23	-0.86±0.04	2.76±0.18
F2	102.90±0.35	-0.94±0.01	3.14±0.13
F3	103.51±0.19	-0.93±0.03	3.14±0.24
F4	103.11±0.42	-0.89±0.00	2.81±0.12
F5	103.21±0.35	-0.89±0.01	2.81±0.12
F6	103.90±0.16	-0.90±0.01	3.12±0.09
F7	104.06±0.64	-1.00±0.00	3.44±0.26
F8	103.63±0.17	-0.93±0.03	3.03±0.21
F9	103.67±0.24	-0.98±0.01	2.88±0.04

**Table 5.** Principal components analysis based on correlation matrix

PC	Eigenvalues	Total variance, %	Eigenvectors		
			$L$	$a^*$	$b^*$
PC1	1.7036	56.7873	-0.4068	0.5925	-0.6953
PC2	0.9559	31.8629	0.8397	0.5423	-0.0292
PC3	0.3405	11.3498	-0.3597	0.5957	0.7181

The factorial loadings plot allows us to identify the variables that have the greatest effect on each component. Factor loadings can range from -1 to 1, with factor loadings near -1 or 1 indicating that the variable strongly influences the component, and factor loadings near 0 indicate that the variable has a weak influence on the component. The factor loadings plot allowed us to infer that the variables  $b^*$  and  $a^*$  had a strong influence on PC1, and  $L^*$  and  $a^*$  on PC2 (Figure 5A).

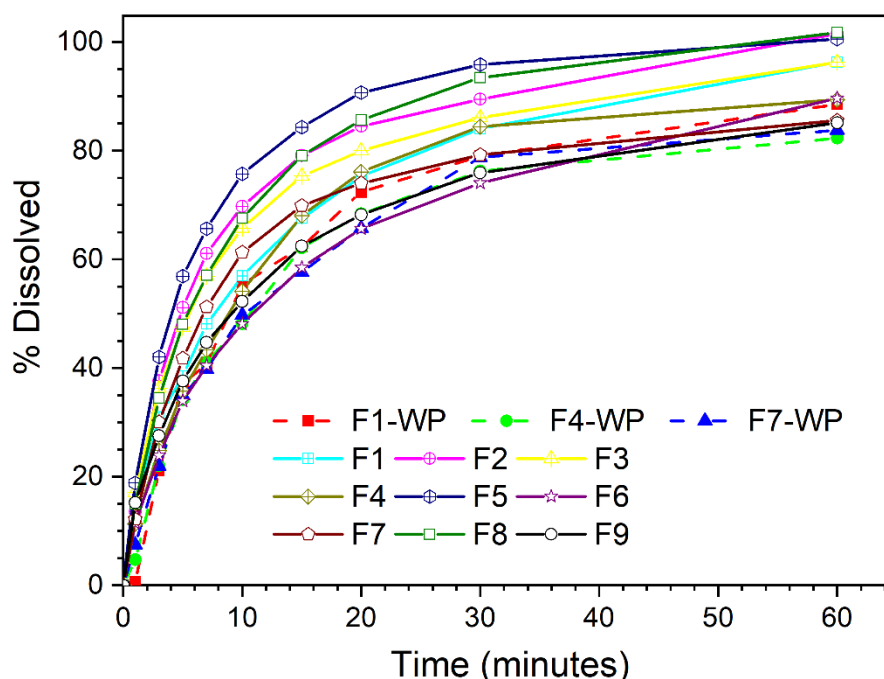
The score plots indicate the color similarities between the samples. Figure 5A shows the projection of the samples in a two-dimensional space formed by the first two principal components (PC1 vs. PC2), which explain 88.65% of the data (Table 5). Standard polystyrene film (SPF), ODF without plasticizers (F1-WP, F4-WP, and F7-WP), and ODFs with plasticizers (F1 and F4) occupied the same region in the score plot, to the right of PC1, with a positive score (region with strong influence of  $a^*$ ), suggesting a similarity between them. When analyzing the samples located at the extremities of PC1 (x-axis), we verified that on the left side was F7, with a negative score, and SPF, with a positive score, indicating a color difference between them. When analyzing PC2 (y-axis), at the bottom of the graph, we found SPF (and F2), with a negative score and, at the top, the other samples, with a positive score (region with strong influence of  $L^*$ , indicating opposite behavior among the samples in relation to PC2). Considering that PC2 has a strong association with  $L^*$ , it can be inferred that, in general, the ODFs did not show the same transparency as SPF.

The initial arcs joining the clusters of the ODFs are compact, with a distance close to zero, suggesting a high similarity between samples. These findings suggest that the addition of a plasticizer does not significantly alter the color of the films. Analyzing the height of the arc formed between the ODFs and the SPF, a large distance between them was observed, suggesting dissimilarity between them (Figure 5B); this fact can be attributed to the presence of CPT.

The results of the clustering and, consequently, the similarity between the samples were analogous to that observed by PCA.

#### Release profiles, kinetic analysis, and model fitting

ODFs prepared without plasticizers (F1-WP, F4-WP and F7-WP) exhibited slower release of CPT than those prepared with plasticizers (F1-9), and ODFs prepared with PP (F2, F5 and F8) showed better release of API (Figure 6).

**Figure 6.** Dissolution profiles of ODFs without plasticizers (F1-WP, F4-WP and F7-WP) and with plasticizers (F1-9)

The dissolution efficiency (DE) (Table 2) is a comparison parameter between dissolution profiles and allows comparison of the time needed for certain drug proportions to be in solution and may be correlated with *in vivo* data [33]. The results of DE were evaluated using DOE; only the plasticizer variable (quadratic) ( $R^2 = 0.85732$ ; Adj: 0.61952) showed a significant influence ( $p < 0.05$ ) and the highest dissolution efficiency was observed for the PP plasticizer.

To establish a relationship between the structure of the polymeric systems and the drug release rate, a study of the release kinetics is of great importance. The release profiles were evaluated using zero-order, first-order, Higuchi, and Korsmeyer-Peppas kinetic models. The model that best fit the API release data was selected based on the correlation coefficient ( $r$ ) of various models.

Zero-order kinetics describe systems where the drug release rate is independent of the concentration of the dissolved substance. The first-order equation can be used to describe the concentration gradients between a static liquid layer and a solid surface or bulk liquid. When the concentration gradient is constant, the surface area of the polymer system remains constant during the dissolution process. However, for a biodegradable polymeric matrix, disintegration occurs during the dissolution process, and the surface area generated varies with time. The first mathematical model used to describe drug release from a matrix system was the Higuchi model, which considers drug release as a diffusion process based on the following hypotheses: the initial drug concentration in the matrix is much higher than drug solubility, drug diffusion takes place only in one dimension, drug particles are much smaller than drug delivery system thickness, matrix swelling, dissolution are negligible, drug diffusivity is constant, and perfect sink conditions are always attained in the release environment. The Korsmeyer-Peppas model describes the release of compounds from polymeric supports through the Fick diffusion process. In this model, the proportionality constant  $k$  incorporates the structural and geometric features of the polymeric system, and the release exponent  $n$  characterizes the diffusion mechanism of the API [34]. When  $n \leq 0.5$  or  $n \geq 1$ , the diffusion mechanism is considered a Fick model, where there is dependence only on the intumescence of the material and the diffusion of the compound into the medium. These two cases differ only in the time dependence, where for  $n \geq 1$ , there is a zero-order time-independent release. For the cases where  $0.5 < n \leq 1$ , the diffusion model is considered anomalous and not Fickian, where the diffusion of the compounds does not solely depend on the intumescence of the material but also suffers interference from other factors such as matrix degradation [39].

According to the Korsmeyer-Peppas kinetic model,  $r$  values indicated a greater adequacy of the release profiles (Table 6). The values of  $n$  indicate that the release mechanism was anomalous (non-Fickian) and controlled by a combination of diffusion, polymer relaxation, and erosion processes. The increase in the constant  $k$  as a function of polymer concentration in ODFs prepared without plasticizers, and its change as a function of the addition of different plasticizers suggests that the release kinetics are favored by the morphological modifications promoted by the plasticizers in the matrix.

**Table 6.** Model dependent kinetic analysis of the dissolution profiles

Samples	Zero Order		First Order		Higuchi model		Korsmeyer-Peppas model		
	$r$	$k_0$	$r$	$k_1$	$r$	$k_H$	$r$	$k_{KP}$	$n$
F1-WP	0.9780	2.1713	0.9766	3.0875	0.9840	4.6628	0.9887	2.6153	0.6863
F4-WP	0.9661	2.3388	0.9899	3.0834	0.9925	4.6576	0.9957	2.6660	0.6603
F7-WP	0.9782	2.2448	0.9909	3.0918	0.9933	4.6468	0.9956	3.0204	0.5952
F1	0.9649	2.2063	0.9937	3.0883	0.9975	4.6551	0.9993	3.9902	0.5575
F2	0.9284	2.2339	0.9701	3.0664	0.9896	4.6671	0.9981	4.1412	0.6843
F3	0.9585	2.1354	0.9773	3.0884	0.9955	4.6634	0.9996	4.5790	0.5882
F4	0.9745	2.3112	0.9925	3.0789	0.9964	4.6567	0.9998	3.0370	0.6526
F5	0.9548	2.0701	0.9916	3.0377	0.9959	4.6725	0.9997	4.9039	0.6678
F6	0.9508	2.4863	0.9851	3.1052	0.9977	4.6471	0.9991	3.3427	0.5524
F7	0.9751	2.1553	0.9869	3.0611	0.9936	4.6608	0.9990	3.6512	0.6335
F8	0.9683	2.1154	0.9952	3.0526	0.9957	4.6659	0.9993	4.1039	0.6504
F9	0.9606	2.2505	0.9816	3.0865	0.9989	4.6518	0.9995	4.0942	0.5005

$r$  is the correlation coefficient;  $k_0$  is the zero-order release constant,  $k_1$  is the first-order kinetic constant,  $k_H$  represents the Higuchi rate constant,  $k$  is the Korsmeyer-Peppas dissolution rate constant and the  $n$  is the release exponent

### Optimization of ODFs

In recent years, industries have successfully applied experimental planning to improve production efficiency and reduce processing costs without sacrificing the quality of their products. According to Goethals and Cho [40], one of the main difficulties in solving problems of multiple characteristics (multivariate) is to

optimize each of their characteristics simultaneously, and one of the most widely used methods to solve problems of multiple response optimization is the desirability function available in the DoE optimization.

Based on the effects of thickness, mechanical properties (elongation at break, puncture strength, and adhesiveness), disintegration time, and DE of the ODFs, it was possible to select the best formulation based on  $0 \leq f_D \leq 1$ , using the optimal values of all the factors [35]. The maximum value for  $f_D$  was 0.8520, corresponding to 2.0 - 2.5% of the polymer (HPMC E6), and PP as plasticizer (Figure 7).

Dinge and Nagarsenker [41] developed ODFs of triclosan using HPMC as a matrix, and Poloxamer and HP $\beta$ CD as solubilizing agents. They showed that HPMC (Methocel E5 Premium LV) could form films with excellent palatability, good mechanical properties, and adequate dissolution rate at a concentration of 2.2% (w/v).

Rezaee and Ganji [13] developed fast-dissolving films containing CPT with 26% pullulan, 74% HPMC, 1% CNF, and 5% Gly. The in vivo comparison of fast-dissolving films with a conventional captopril sublingual tablet exhibited significant increase in AUC ( $\sim 62\%$ ) and  $C_{max}$  ( $\sim 52\%$ ) and a major decrease in  $T_{max}$  ( $\sim 33\%$ ).

### Profiles for Predicted Values and Desirability

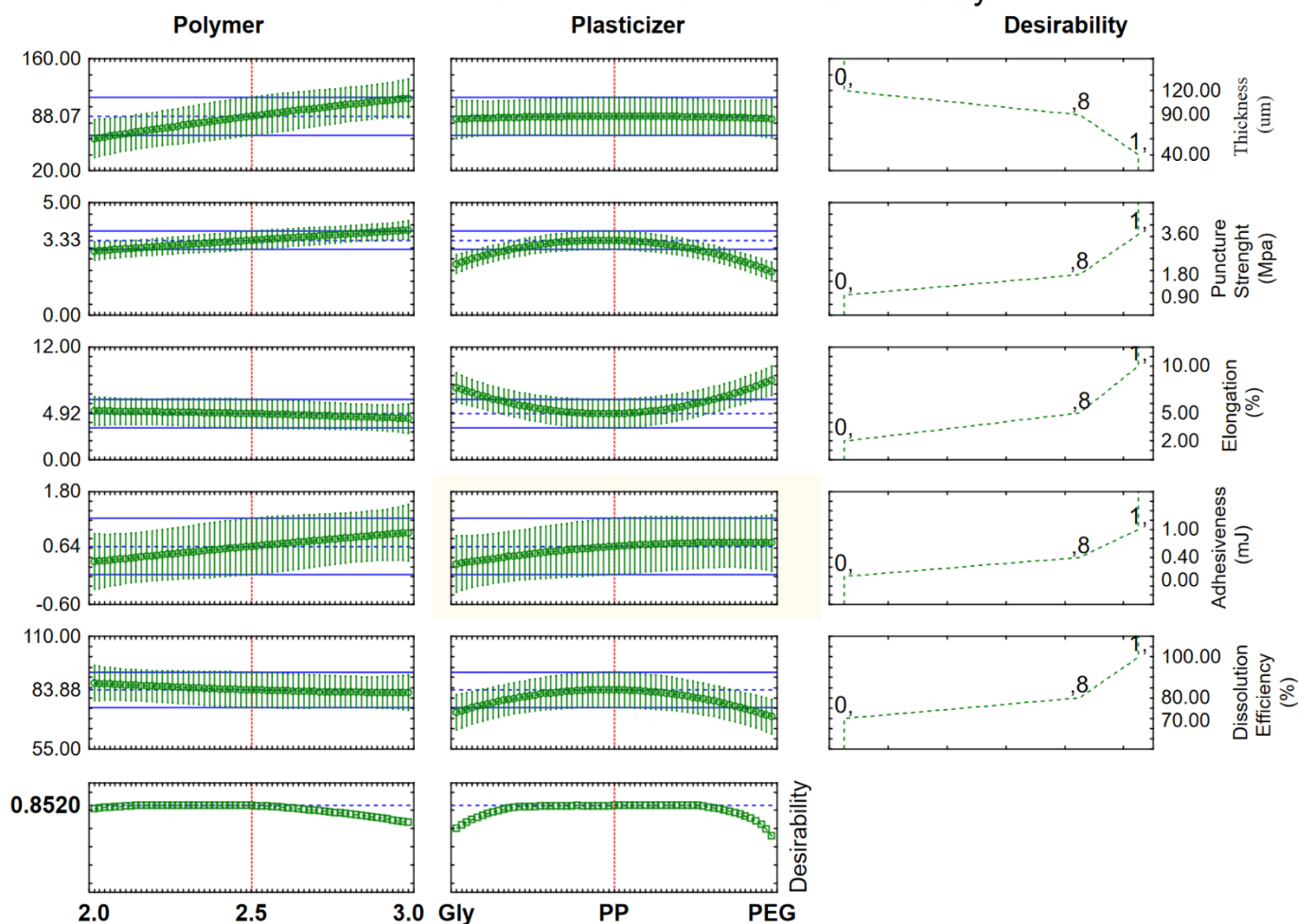


Figure 7. Desirability function ( $f_D = 0.8520$ )

## CONCLUSION

In this study, ODFs containing CPT were prepared using HPMC E6 as the film-forming polymer and Gly, PP, or PEG as the plasticizer.

The amount of HPMC E6 (2% to 3%) and the nature of the plasticizer (Gly, PP, or PEG) played a critical role in the physical, mechanical, and physicochemical properties of ODFs.

Films prepared with Gly or PEG were translucent, whereas those prepared with PP were transparent.

The best-fitting kinetics model for CPT release from the ODFs was the Korsmeyer-Peppas model, and the release mechanism was anomalous (non-Fickian), controlled by a combination of diffusion, polymer relaxation, and erosion processes.

Based on the effects of thickness, disintegration time, mechanical properties (puncture and adhesion tests), and DE values, it was possible to select the best formulation according to the  $f_D$  using the optimal

values of all the factors. The maximum value for the  $f_D$  was 0.8520, corresponding to the application of 2.0 - 2.5% polymer (HPMC E6), and PP as plasticizer.

PCA and HCA allowed us to obtain a more defined distinction of the ODFs according to their chromatic characteristics. Furthermore, DoE successfully facilitated the interpretation of the experimental data and allowed the identification of the optimal values of the factors for maximum yield.

The overall results showed that orally disintegrating films can be a promising alternative for oral administration of captopril.

**Funding:** This research did not receive any specific grant from funding agencies in the public, commercial, or not-for-profit sectors.

**Acknowledgments:** We would like to thank NATEP and NIPE for allowing the use of the equipment (CT3 Texture Analyzer and Jeol JSM-6360LV SEM) and Editage (www.editage.com) for English language editing.

**Conflicts of Interest:** The authors claim that there is no conflict of interest.

## REFERENCES

1. Takeuchi H, Yamakawa R, Nishimatsu T, Takeuchi Y, Hayakawa K, Maruyama N. Design of rapidly disintegrating drug delivery films for oral doses with hydroxypropyl methylcellulose. *J Drug Deliv Sci Technol* [Internet]. 2013;23(5):471–5. Available from: [http://dx.doi.org/10.1016/S1773-2247\(13\)50068-2](http://dx.doi.org/10.1016/S1773-2247(13)50068-2)
2. Williams B, Mancia G, Spiering W, Rosei EA, Azizi M, Burnier M, et al. 2018 practice guidelines for the management of arterial hypertension of the European society of cardiology and the European society of hypertension ESC/ESH task force for the management of arterial hypertension. *J. Hypertens.* 2018;36:2284–309.
3. De Souza MC, Diniz LF, de Jesus Franco CH, de Abreu HA, Diniz R. Structural study of the stability of the captopril drug regarding the formation of its captopril disulphide dimer. *J Struct Chem.* 2016;57(6):1111–20.
4. Alipour S, Mohammadi A, Ahmadi F. Captopril fast disintegrating tablets for children: formulation and quality control by HPLC. *Trends Pharm Sci* [Internet]. 2017;3(3). Available from: <http://tips.sums.ac.ir/index.php/TiPS/article/view/144>
5. Huang Y Bin, Tsai YH, Chang JS, Liu JC, Tsai MJ, Wu PC. Effect of antioxidants and anti-irritants on the stability, skin irritation and penetration capacity of captopril gel. *Int J Pharm.* 2002;241(2):345–51.
6. Pabari RM, McDermott C, Barlow J, Ramtoola Z. Stability of an Alternative Extemporaneous Captopril Fast-Dispersing Tablet Formulation Versus an Extemporaneous Oral Liquid Formulation. *Clin Ther* [Internet]. 2012;34(11):2221–9. Available from: <http://dx.doi.org/10.1016/j.clinthera.2012.10.005>
7. Tôrres AR, Grangeiro S, Fragoso WD. Vibrational spectroscopy and multivariate control charts: A new strategy for monitoring the stability of captopril in the pharmaceutical industry. *Microchem J.* 2017;133:279–85.
8. Borges AF, Silva C, Coelho JFJ, Simões S. Oral films: Current status and future perspectives II-Intellectual property, technologies and market needs. *J Control Release* [Internet]. 2015;206:108–21. Available from: <http://dx.doi.org/10.1016/j.jconrel.2015.03.012>
9. Lee Y, Kim K, Kim M, Choi DH, Jeong SH. Orally disintegrating films focusing on formulation, manufacturing process, and characterization. *J Pharm Investig* [Internet]. 2017;47(3):183–201. Available from: <http://10.03.239/s40005-017-0311-2>
10. Preis M, Knop K, Breikreutz J. Mechanical strength test for orodispersible and buccal films. *Int J Pharm* [Internet]. 2014 Jan;461(1–2):22–9. Available from: <http://dx.doi.org/10.1016/j.ijpharm.2013.11.033>
11. Siddiqui M, Garg G, Sharma P. A Short Review on “A Novel Approach in Oral Fast Dissolving Drug Delivery System and Their Patents.” *Adv Biol Res.* 2010;5.
12. Singh H, Kaur M, Verma H. Optimization and Evaluation of Desloratadine Oral Strip: An Innovation in Paediatric Medication. Concheiro A, Nekam K, editors. *Sci World J* [Internet]. 2013;2013:395681. Available from: <https://doi.org/10.1155/2013/395681>
13. Rezaee F, Ganji F. Formulation, Characterization, and Optimization of Captopril Fast-Dissolving Oral Films. *AAPS PharmSciTech.* 2018;19(5):2203–12.
14. Chauhan K, Solanki R, Sharma S. A review on fast dissolving tablet. *Int. J. Appl. Pharm.* 2018.
15. Chonkar AD, Bhagawati ST, Udupa N. An Overview on Fast Dissolving Oral Films. *Asian J Pharm Technol.* 2015;
16. Mahadevaiah, Shivakumara LR, Demappa T, Vasudev S. Mechanical and Barrier Properties of Hydroxy Propyl Methyl Cellulose Edible Polymer Films with Plasticizer Combinations. *J Food Process Preserv.* 2017;41(4):1–10.
17. Dixit RP, Puthli SP. Oral strip technology: Overview and future potential. *J Control Release.* 2009 Oct;139(2):94–107.
18. Raymond C Rowe, Paul J Sheskey MEQ. *Handbook of Pharmaceutical Excipients.* 6 ed. Revue des Nouvelles Technologies de l'Information. 2015.
19. Morales JO, McConville JT. Manufacture and characterization of mucoadhesive buccal films. *Eur J Pharm Biopharm Off J. Arbeitsgemeinschaft fur Pharm Verfahrenstechnik eV* [Internet]. 2011 Feb;77(2):187–99. Available from: <http://dx.doi.org/10.1016/j.ejpb.2010.11.023>
20. Rani NS, Sannappa J, Demappa T, Mahadevaiah. Structural and ionic conductivity behavior in hydroxypropylmethylcellulose (HPMC) polymer films complexed with sodium iodide (NaI). In: *AIP Conference Proceedings.* 2013.

21. Ali SI, Jahangir MA, Ahmed MM, Muheem A, Shahab MS, Bhavani PD, et al. Development and in vitro evaluation of mouth dissolving films of captopril. *Int Res J Pharm* [Internet]. 2015 Nov 30;6(11):760–4. Available from: [http://www.irjponline.com/admin/php/uploads/2432\\_pdf.pdf](http://www.irjponline.com/admin/php/uploads/2432_pdf.pdf)
22. Uhoraningoga A, Kinsella GK, Henehan GT, Ryan BJ. The goldilocks approach: A review of employing design of experiments in prokaryotic recombinant protein production. *Bioengineering*. 2018 Oct;5(4).
23. Bharti K, Mittal P, Mishra B. Formulation and characterization of fast dissolving oral films containing buspirone hydrochloride nanoparticles using design of experiment. *J Drug Deliv Sci Technol* [Internet]. 2019 Feb 1 [cited 2021 May 21];49(December 2018):420–32. Available from: <https://doi.org/10.1016/j.jddst.2018.12.013>
24. Musazzi UM, Khalid GM, Selmin F, Minghetti P, Cilurzo F. Trends in the production methods of orodispersible films. *Int J Pharm*. 2020 Feb;576:118963.
25. Karki S, Kim H, Na S-JJ, Shin D, Jo K, Lee J. Thin films as an emerging platform for drug delivery. *Asian J Pharm Sci* [Internet]. 2016;11(5):559–74. Available from: <http://dx.doi.org/10.1016/j.ajps.2016.05.004>
26. ASTM D6132-13(2017). ASTM D6132-13(2017). Stand Test Method Nondestruct Meas Dry Film Thick Appl Org Coatings Using an Ultrason Coat Thick Gage [Internet]. Available from: <https://www.astm.org/Standards/D6132.htm>
27. ASTM D2582 - 16. In: Standard Test Method for Puncture-Propagation Tear Resistance of Plastic Film and Thin Sheeting [Internet]. Available from: <https://www.astm.org/Standards/D2582.htm>
28. ASTM D4541 - 17. In: Standard Test Method For Pull-Off Strength Of Coatings Using Portable Adhesion Testers [Internet]. Available from: <https://www.astm.org/Standards/D4541.htm>
29. Radebaugh GW, Murtha JL, Julian TN, Bondi JN. Methods for evaluating the puncture and shear properties of pharmaceutical polymeric films. *Int J Pharm* [Internet]. 1988;45(1):39–46. Available from: <https://www.sciencedirect.com/science/article/pii/0378517388900324>
30. Carvalho FC, Bruschi ML, Evangelista RC, Gremião MPD. Mucoadhesive drug delivery systems [Internet]. *Brazilian Journal of Pharmaceutical Sciences Universidade de São Paulo, Faculdade de Ciências Farmacêuticas*; Mar, 2010 p. 1–17. Available from: [http://www.scielo.br/scielo.php?script=sci\\_arttext&pid=S1984-82502010000100002&lng=en&tng=en](http://www.scielo.br/scielo.php?script=sci_arttext&pid=S1984-82502010000100002&lng=en&tng=en)
31. Takeuchi Y, Kawamoto M, Tahara K, Takeuchi H. Design of a new disintegration test system for the evaluation of orally disintegrating films. *Int J Pharm* [Internet]. 2018 Dec 20 [cited 2021 Feb 26];553(1–2):281–9. Available from: <https://doi.org/10.1016/j.ijpharm.2018.10.049>
32. Krampe R, Sieber D, Pein-Hackelbusch M, Breitreutz J. A new biorelevant dissolution method for orodispersible films. *Eur J Pharm Biopharm* [Internet]. 2016 Jan 1 [cited 2021 Jun 16];98(October):20–5. Available from: <http://dx.doi.org/10.1016/j.ejpb.2015.10.012>
33. Simionato LD, Petrone L, Baldut M, Bonafede SL, Segall AI. Comparison between the dissolution profiles of nine meloxicam tablet brands commercially available in Buenos Aires, Argentina. *Saudi Pharm J*. 2018;
34. Lee M-W, Yang T-P, Peng H-H, Chen J-W. Preparation and characterization of polygalacturonic acid/rosmarinic acid membrane crosslinked by short chain hyaluronate for preventing postoperative abdominal adhesion. *Carbohydr Polym*. 2012;87:1749–55.
35. Vera Candiotti L, De Zan MM, Cámara MS, Goicoechea HC. Experimental design and multiple response optimization. Using the desirability function in analytical methods development. *Talanta* [Internet]. 2014 Jun 15 [cited 2021 Feb 11];124:123–38. Available from: <https://www.sciencedirect.com/science/article/pii/S0039914014000459>
36. Santana RF, Bonomo RCF, Gandolfi ORR, Rodrigues LB, Santos LS, dos Santos Pires AC, et al. Characterization of starch-based bioplastics from jackfruit seed plasticized with glycerol. *J Food Sci Technol*. 2018.
37. Sothornvit R, Krochta JM. Plasticizer effect on oxygen permeability of beta-lactoglobulin films. *J Agric Food Chem*. 2000 Dec;48(12):6298–302.
38. Tuberoso CIG, Jerković I, Sarais G, Congiu F, Marijanović Z, Kuš PM. Color evaluation of seventeen European unifloral honey types by means of spectrophotometrically determined CIE L\**a*\**b*° chromaticity coordinates. *Food Chem*. 2014;145:284–91.
39. Siepman J, Siepman F. Mathematical modeling of drug delivery. *Int J Pharm*. 2008 Dec;364(2):328–43.
40. Goethals PL, Cho BR. Extending the Desirability Function to Account for Variability Measures in Univariate and Multivariate Response Experiments. *Comput Ind Eng* [Internet]. 2012 Mar 1 [cited 2021 Feb 11];62(2):457–68. Available from: <https://doi.org/10.1016/j.cie.2011.10.012>
41. Dinge A, Nagarsenker M. Formulation and evaluation of fast dissolving films for delivery of triclosan to the oral cavity. *AAPS PharmSciTech*. 2008;



© 2022 by the authors. Submitted for possible open access publication under the terms and conditions of the Creative Commons Attribution (CC BY NC) license (<https://creativecommons.org/licenses/by-nc/4.0/>).